frontiers in Communications and Networks

ORIGINAL RESEARCH
published: 13 May 2021
doi: 10.3389/frcmn.2021.672857

Reconfigurable Intelligent Surfaces for Doppler Effect and Multipath Fading Mitigation

*Ertugrul Basar**

Communications Research and Innovation Laboratory, Department of Electrical and Electronics Engineering, Koç University, Istanbul, Turkey

Owing to the envisioned new use-cases, such as immersive virtual reality and high-fidelity mobile hologram, and their potential challenging new requirements for future wireless networks, extensive research has already started on 6G and beyond wireless technologies. Despite the fact that several modern physical layer solutions have been introduced in the past decade, a level of saturation has been reached in terms of the available spectrum and adapted modulation/coding solutions, which accordingly limits the maximum capacity and reliability. Within this respective, reconfigurable intelligent surface (RIS)-empowered communication appears as a potential candidate to overcome the inherent drawbacks of legacy wireless systems. The core idea of RIS-assisted communication is the transformation of the random and uncontrollable wireless propagation environment into a reconfigurable communication system entity that plays an active role in conveying information and improving system performance. In this paper, the well-known multipath fading phenomenon is revisited in mobile wireless communication systems, and novel and unique solutions are introduced from the perspective of RISs. The feasibility of eliminating or mitigating the multipath fading effect stemming from the movement of mobile receivers is also investigated by utilizing RISs. It is shown that rapid fluctuations in the received signal strength due to the Doppler effect can be effectively reduced by using real-time tunable RISs. It is also proven that for a hypothetical propagation environment where all reflectors are coated with RISs, the multipath fading effect can be totally eliminated. Furthermore, we show that for more general propagation environments with several interacting objects, even a few real-time tunable RISs can remarkably reduce the Doppler spread and the deep fades in the received signal.

Keywords: 6G, Doppler effect, multipath fading, reconfigurable intelligent surface, intelligent reflecting surface

OPEN ACCESS

Edited by:
Abdulkadir Celik,
King Abdullah University of Science and Technology, Saudi Arabia

Reviewed by:
Anas M. Salhab,
King Fahd University of Petroleum and Minerals, Saudi Arabia
Shuaishuai Guo,
Shandong University, China
Qurrat-Ul-Ain Nadeem,
University of British Columbia Okanagan, Canada

***Correspondence:**
Ertugrul Basar
ebasar@ku.edu.tr

Specialty section:
This article was submitted to Wireless Communications, a section of the journal Frontiers in Communications and Networks

Received: *26 February 2021*
Accepted: *13 April 2021*
Published: *13 May 2021*

Citation:
Basar E (2021) Reconfigurable Intelligent Surfaces for Doppler Effect and Multipath Fading Mitigation. Front. Comms. Net. 2:672857. doi: 10.3389/frcmn.2021.672857

1. INTRODUCTION

Fifth generation (5G) wireless networks have three major use-cases with different user requirements, namely enhanced mobile broadband (eMBB), ultra-reliable and low-latency communications (URRLC), and massive machine type communications (mMTC). Although the introduction of promising physical layer (PHY) technologies in 5G, including millimeter wave (mmWave) communications, massive multiple-input multiple-output (MIMO) systems with hybrid precoding, and multiple orthogonal frequency division multiplexing (OFDM)

numerologies, the most recent mobile communication standards do not contain revolutionary ideas in terms of PHY solutions. Within this context, researchers have already started research on next-generation (6G) mobile technologies of 2030 and beyond by exploring completely new and radical PHY concepts to satisfy the requirements of the envisioned science-fiction like technologies. Although future 6G technologies might seem to be extensions of their 5G counterparts at this time (Gatherer, 2018), potential new user requirements, challenging use-cases, and new networking trends of 6G (Saad et al., 2020) will bring more challenging problems in mobile wireless communication, which necessitate radically new PHY concepts for next-generation radios. New solutions for 6G any beyond must provide extremely high energy and spectral efficiencies along with ultra-reliability and ultra-security. Furthermore, we need a highly flexible and controllable PHY concept to satisfy the challenging requirements of the envisioned use-cases. Despite the intensive research efforts in the field of PHY research during the past two decades, these are still features that we seek for in state-of-the-art wireless communication systems and standards, which might necessitate a rethink of communication system design for 6G and beyond.

Due to the random and uncontrollable behavior of wireless propagation, it has always been challenging for the network operators to build ubiquitous wireless networks that can provide high quality-of-service (QoS) and uninterrupted connectivity to multiple users and devices in the presence of harsh propagation environments since the early wireless networks (Molisch, 2011). Particularly, this challenging behavior of wireless propagation causes

(i) *deep fading* due to uncontrollable interactions of transmitted waves with surrounding objects and their constructive and destructive interference at the receiver,
(ii) *severe attenuation* due to high path loss and transmissions under blocked line-of-sight (LOS) links (shadowing),
(iii) *inter-symbol interference* due to different runtimes of multipath components relative to the symbol period, and
(iv) *Doppler effect* due to the high mobility of users and/or surrounding objects.

Although a plethora of modern PHY solutions, including multi-carrier modulation, adaptive modulation and coding, non-orthogonal multiple access, relaying, beamforming, massive MIMO, and reconfigurable antennas, have been considered to overcome these challenges in the next several decades, the overall progress in terms of the PHY improvement has been still relatively slow. This can be explained by the following undeniable fact in wireless systems: *the propagation environment has been perceived as a randomly behaving entity until the start of the modern wireless communications era and it degrades the overall received signal quality and the communication QoS owing to the uncontrollable interactions of the transmitted signals with the surrounding objects*. In other terms, the primary focus of system designers has always been the transmitter and receiver ends of communication systems to cope with the negative effect of the wireless channel, which is inherently assumed to an uncontrollable part of communication systems. One of the main objectives of this paper is to challenge this view by exploiting the new paradigm of intelligent communication environments.

In recent years, reconfigurable intelligent surfaces (RISs) have been brought to the attention of the wireless research community to enable the control of wireless environments (Basar et al., 2019; Di Renzo, 2019). RISs are artificial and 2D surfaces of electromagnetic (EM) material that are electronically controlled with integrated electronics. By modifying the current distribution over themselves in a deliberate manner, RISs might support unique EM functionalities, including anomalous reflection, wave absorption, polarization modification, wave splitting, wave focusing, and phase modification. Recent practical efforts in the literature have revealed that these unique EM functionalities are possible with a very simple architecture that does not require complex decoding, encoding, and radio frequency (RF) processing operations and the communication QoS (capacity, signal power, secrecy, error performance, etc.) can be boosted by exploiting the implicit randomness of wireless propagation (Basar et al., 2019). However, the fundamental issues remain unsolved within the theoretical and practical understanding as well as modeling of RIS-aided communication systems.

Contrary to traditional wireless networks, where the wireless communication environment is out of control of the system designers, the emerging concept of smart radio environments have been realized by RISs. Here, the propagation environment is turned into an intelligent and controllable system entity that plays an active role in processing signals and accordingly, transferring information in an effective way. It is worth noting that the introduction of controllable propagation is a completely new paradigm in wireless communication and has the potential to change the way the communication takes place. The core technology behind this new concept is RISs, which are the 2D equivalent of metamaterials (metasurfaces). It is worth noting that RIS-empowered communication is completely different from other well-known technologies, such as MIMO beamforming, amplify-and-forward relaying, passive reflect-arrays, and backscatter communications, which are currently employed in wireless networks. On the other hand, RIS-assisted systems have the following major distinguishable features and advantages:

(i) RISs do not require an energy source for RF signal processing thanks due their almost passive architecture;
(ii) RISs provide an inherently full-duplex transmission and do not amplify or introduce noise when reflecting the signals due to their passive natures;
(iii) RISs can be easily deployed on certain locations, such as the facades of buildings, ceilings of factories, and indoor walls;
(iv) RISs are reconfigurable and can adapt themselves according to the changes of the wireless environment.

These distinctive characteristics make RIS-empowered communication a unique technology and introduce important communication theoretical as well as system design challenges, some of which will be tackled in this paper.

Within the context of radical PHY solutions toward beyond 5G wireless networks, there has been a growing recent interest

in novel signaling and modulation concepts in which the propagation environment is controlled or its inherently random nature is exploited to further increase the spectral/energy efficiency and/or QoS of target communication systems. For instance, IM-based (Basar, 2016; Basar et al., 2017) schemes, such as media-based modulation (Khandani, 2013; Basar, 2019a) and spatial scattering modulation (Ding et al., 2017) benefit from reconfigurable antennas or scatterers in the environment to create different signatures for received signals in rich scattering environments and transmit additional information bits accordingly. On the other hand, RISs primarily focus on the control of the propagation environment by exploiting reconfigurable reflectors/scatterers embedded on themselves to boost the signal quality at the receiver. It is worth noting that a number of preliminary works have been reported in the earlier literature to control or benefit from wireless propagation, such as intelligent walls (Subrt and Pechac, 2012a,b), spatial microwave modulators (Kaina et al., 2014), 3D reflectors (Xiong et al., 2017), and coding metamaterials (Cui et al., 2014). Nevertheless, the rise of RIS-empowered intelligent communication environments can be mainly attributed to programmable (digitally-controlled) metasurfaces (Yang et al., 2016), reconfigurable reflect-arrays (Tan et al., 2016, 2018), software-controlled hypersurfaces (Liaskos et al., 2018), and intelligent metasurfaces (Liu et al., 2019). For instance, the intelligent metasurface design of Liu et al. (2019), enables tunable anomalous reflection as well as perfect absorption by carefully adjusting the resistance and the capacitance of its unit cells at 5 GHz.

The concept of RIS-empowered wireless communication has received tremendous interest from researchers in our community in the past couple of years due to interesting as well as challenging problems it brings in the context of metamaterials and electromagnetics, communication, optimization, and probability theories (Basar et al., 2019; Di Renzo, 2019; Wu and Zhang, 2019b; Di Renzo et al., 2020). Particularly, researchers focused on

(i) maximization of the achievable rate, minimum signal-to-interference-plus noise ratio (SINR), and energy efficiency and minimization of the transmit power by joint optimization of the RIS phases and the transmit beamformer (Huang et al., 2018a,b, 2019; Wu and Zhang, 2018; Yu et al., 2019b; Nadeem et al., 2020),
(ii) maximization of the received signal-to-noise ratio (SNR) to minimize the symbol error probability (Basar, 2019b),
(iii) efficient channel estimation techniques with passive RIS elements as well as deep learning tools to reduce the training overhead and to reconfigure RISs (Mishra and Johansson, 2019; He and Yuan, 2020; Taha et al., 2021),
(iv) PHY security solutions by joint optimization of the transmit beamformer and RIS phases (Chen et al., 2019; Cui et al., 2019; Yu et al., 2019a),
(v) practical issues, such as erroneous reflector phases, realistic phase shifts, and discrete phase shifts (Wu and Zhang, 2019a; Abeywickrama et al., 2020; Badiu and Coon, 2020),
(vi) design of NOMA-based systems for downlink transmit power minimization and for the minimum decoding SINR maximization of all users (Ding and Poor, 2019; Fu et al., 2019),
(vii) channel modeling and measurements for different frequency bands and RIS types (Tang, 2019; Basar and Yildirim, 2020a,b,c; Danufane et al., 2020; Yildirim et al., 2020), and
(viii) practical implementations (Dai et al., 2020, 2021).

Furthermore, the first attempts on combining RISs with space modulation, visible light and free space optical communications, unmanned aerial vehicles, wireless information and power transfer systems, and OFDM systems have been reported in recent times (see Basar et al., 2019; Di Renzo et al., 2020; Wu et al., 2020 and references therein).

In our paper, we take a step back and revisit the well-known phenomenons of multipath fading and Doppler effect in mobile communications from the perspective of emerging RISs. Although the potential of RISs has been explored from many aspects as discussed above, to the best of our knowledge, their potential in terms of Doppler effect mitigation has not been fully understood yet. For this purpose, by following a bottom-up approach from simple networks to more sophisticated ones, we explore the potential of RISs to eliminate multipath fading effect stemming from Doppler frequency shifts of a mobile receiver for the first time in the literature. Specifically, we prove that the rapid fluctuations in the received signal strength due to the user movement can be effectively eliminated and/or mitigated by utilizing real-time tunable RISs. We introduce a number of novel and effective methods that provide interesting trade-offs between Doppler effect mitigation and average received signal strength maximization, for the reconfiguration of the available RISs in the system and reveal their potential for future mobile networks.

It is worth noting that the results in this paper are obtained for hypothetical RISs which create specular reflections with a single and very large conducting element. However, the results obtained in this paper can be adapted for practical RISs in which many number of tiny elements on them scatter the incoming signals in all directions, in other words, for RISs with multiplicative path loss terms. Finally, it has been also shown that by using carefully positioned and relatively large RISs, it might be possible to reach the same path gain as that of specular reflection by carefully adjusting the phases of RIS elements (Ellingson, 2019). Nevertheless, exploration of application scenarios in which practical RISs might be effectively used to overcome Doppler and multipath effects is an open problem and this paper aims to shed light in this direction by following a unified signal processing perspective.

The rest of the paper is organized as follows. In section 2, we consider a simple two-path scenario and revisit multipath and Doppler effects. In section 3, we deal with Doppler effect elimination with RISs. More sophisticated networks with multiple RISs and objects as well as practical issues are covered under **Supplementary Material**. Finally, we conclude the paper in section 4.

2. REVISITING MULTIPATH AND DOPPLER EFFECTS WITH SIMPLE CASE STUDIES

In this section, we revisit the Doppler and multipath fading effects caused by the movement of a mobile receiver under a simple propagation scenario (with and without an RIS). We focus our attention to the low-pass equivalent and noise-free received signals while a generalization to pass-band signaling is straightforward from the given low-pass equivalent signals.

2.1. Multipath Fading Due to User Movement and A Reflector

In this subsection, we focus on the basic two-path propagation geometry given in **Figure 1** with a base station (BS), a mobile station (MS) and an interacting object (IO) (Basar, 2020). In this geometry, the MS has a constant speed of V (in m/s) and it follows a straight route toward the IO. Here, a second replica of the transmitted signal, reflected from the IO, arrives at the receiver of the MS in addition to the signal traveled through the LOS path between two terminals. For simplicity, a reflection coefficient of unity magnitude and phase π is assumed for the IO, that is, $R = -1$. In this setup, the reflecting surface is assumed to be large and smooth enough to create specular reflections.

To capture the effects of multipath fading and Doppler in the received signal with respect to the motion of the MS in time, the transmission of an unmodulated radio frequency (RF) carrier signal $\cos(2\pi f_c t + \Theta_0)$ is assumed, where f_c is the carrier frequency and Θ_0 is the initial phase. This carrier signal is equivalent to $x(t) = \exp(j\Theta_0)$ in complex baseband representation. Here, we focus on a very short travel distance (a few wavelengths) in order to illustrate the fade pattern and the Doppler spectrum due to the movement of the MS. As a result, the received direct and reflected signals have almost constant amplitudes during our observation, while experiencing rapidly varying phase terms. In other words, focusing on a very short time interval ensures that the large-scale fading does not affect the received signal. At the same time, we observe Doppler shifts at the received signals due to the movement of the MS. Against this background, we obtain the received complex envelope as (Fontan and Espineira, 2008).

$$r(t) = \frac{\lambda}{4\pi}\left(\frac{e^{-j\frac{2\pi d_{\mathrm{LOS}}(t)}{\lambda}}}{d_{\mathrm{LOS}}(t)} - \frac{e^{-j\frac{2\pi d_R(t)}{\lambda}}}{d_R(t)}\right) \tag{1}$$

where the initial carrier phase Θ_0 is dropped for clarity. Here $d_{\mathrm{LOS}}(t)$ and $d_R(t)$, respectively denote the time-varying radio path distances for the BS-MS and the BS-IO-MS links due to the movement of the MS. For this specific setup in **Figure 1**, we have $d_{\mathrm{LOS}}(t) = d_{\mathrm{LOS}} + Vt$ and $d_R(t) = d_{\mathrm{LOS}} + 2d_1 - Vt$, where d_{LOS} and d_1, respectively stand for the initial BS-MS and MS-IO distances. We further assume a horizontal communication link between the BS and the MS owing to their sufficiently small antenna height differences. The same assumption applies to the reflected signal stemming from the IO. In other words, MS travel distance variations directly affect radio path lengths of both rays. However, a generalization is straightforward for signals coming from different angles (see **Supplementary Section 1**). As mentioned earlier, we focus into only a few wavelengths of travel distance of the MS (a very short time interval) to purely focus on small-scale fading effects, while due to this short distance, two rays have approximately constant amplitudes for all positions of the MS. In light of these assumptions in the system model, (1) simplifies to

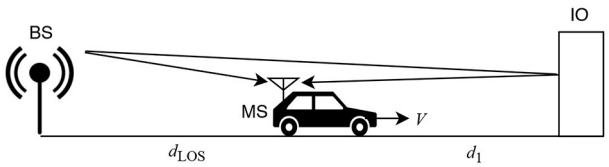

FIGURE 1 | Two-ray propagation model with a mobile station and an IO creating reflections.

$$r(t) = \frac{\lambda}{4\pi}\left(\frac{e^{-j2\pi f_D t - j\phi_{\mathrm{LOS}}}}{d_{\mathrm{LOS}}} - \frac{e^{j2\pi f_D t - j\phi_1}}{d_{\mathrm{LOS}} + 2d_1}\right) \tag{2}$$

where $f_D = V/\lambda$ is Doppler shift with respect to the nominal carrier frequency in the passband or with respect to 0 Hz in low-pass equivalent representation, $\phi_{\mathrm{LOS}} = 2\pi d_{\mathrm{LOS}}/\lambda$, and $\phi_1 = 2\pi(d_{\mathrm{LOS}} + 2d_1)/\lambda$. The constant (initial) phase terms of ϕ_{LOS} and ϕ_1 can be readily dropped if they are integer multiples of 2π. In light of this, using the properties of complex exponentials,[1] the magnitude of the complex envelope can be obtained as follows:

$$|r(t)| = \left(\frac{\lambda}{4\pi}\right)\left(\frac{1}{d_{\mathrm{LOS}}^2} + \frac{1}{(d_{\mathrm{LOS}} + 2d_1)^2} - \frac{2\cos(4\pi f_D t)}{d_{\mathrm{LOS}}(d_{\mathrm{LOS}} + 2d_1)}\right)^{1/2}. \tag{3}$$

In **Figure 2**, the magnitude of the complex envelope in (3) is plotted for the travel of the MS for six wavelengths (which corresponds to an observation time of 0.06 s for the given MS speed) considering the following system parameters[2]: $f_c = 3$ GHz, $V = 10$ m/s with different d_{LOS} and d_1 values for a fixed BS-IO total distance of $d_{\mathrm{LOS}} + d_1 = 2,000$ m. As seen from **Figure 2**, the received signal strength fluctuates rapidly around a mean value that is dictated by the path loss, due to the destructive and constructive interference of arriving two signals. We further note that this fluctuation in the signal envelope has a frequency of $2f_D$ Hz as evident from (3). This oscillation is also known as the *fade pattern* of the received signal's envelope. We also note that the variation of the magnitude is more significant for smaller d_1 values, when the values of $d_{\mathrm{LOS}}(t)$ and $d_R(t)$ are close to each other, which corresponds a stronger interference between multipaths. This is also verified by the Doppler spectrum

[1]For $z_1 = r_1 e^{j\xi_1}$, $z_2 = r_2 e^{j\xi_2}$, and $z_3 = z_1 + z_2 = r_3 e^{j\xi_3}$, we have $r_3 = (r_1^2 + r_2^2 + 2r_1 r_2 \cos(\xi_1 - \xi_2))^{1/2}$.

[2]The same simulation parameters (mobile speed, carrier frequency, observation interval, traveled distance, FFT size, sampling distance and time) are used in the following unless specified otherwise.

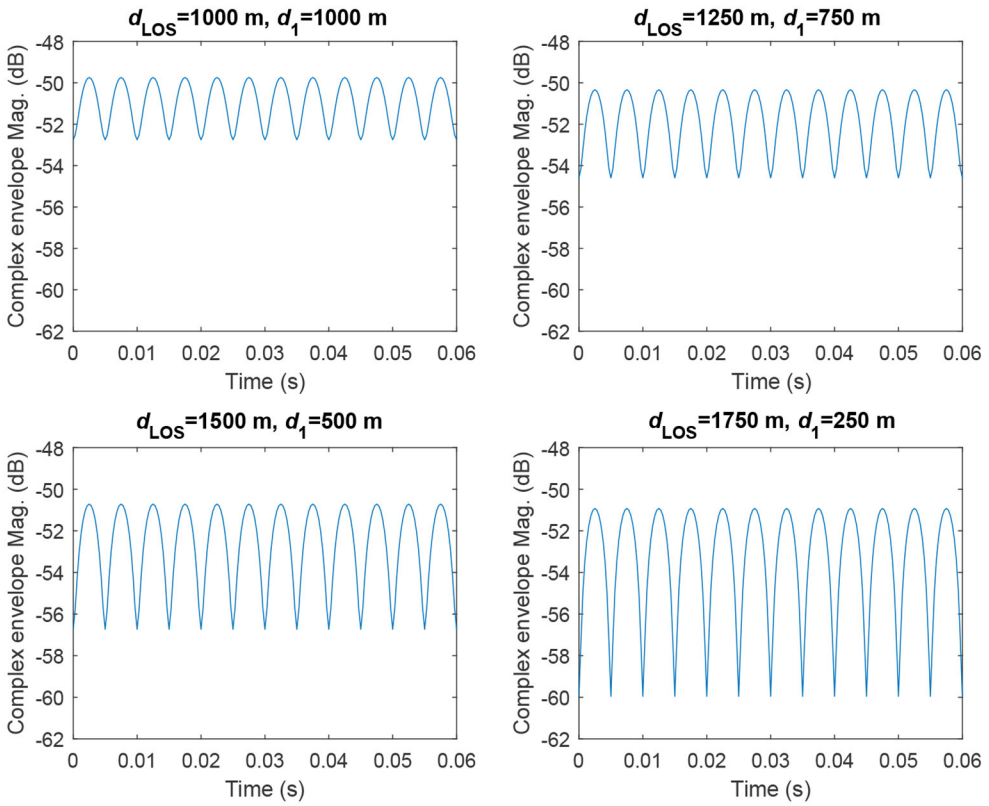

FIGURE 2 | Complex envelope variation with respect to MS movement with $V = 10$ m/s for varying d_{LOS} and d_1 (observation interval: 0.06 s, traveled distance: $6\lambda = 0.6$ m).

of the received signal given in **Figure 3** for these four cases, which include two sharp components at opposite frequencies, i.e., $-V/\lambda = -100$ Hz (from the LOS path) and $V/\lambda = 100$ Hz (from the IO) with different normalized amplitudes due to different travel distances of the two rays.

2.2. Eliminating Multipath Fading Due to User Movement With an RIS

In this subsection, we focus on the same basic system model of subsection 2.1 (**Figure 1**), however, we consider that the IO creates a controllable reflection at this time, thanks to the RIS that is mounted on its facade with the purpose of manipulating the reflected signals. In this setup, we capture the intelligent reflection from the RIS by a time-varying but unit gain (passive) reflection coefficient, which is denoted by $R(t) = e^{j\theta(t)}$. Here $\theta(t)$ stands for the time-varying reflection phase of the RIS. In light of this, the received complex envelope is expressed as

$$r(t) = \frac{\lambda}{4\pi}\left(\frac{e^{-j2\pi f_D t}}{d_{\text{LOS}}} + \frac{e^{j2\pi f_D t + j\theta(t)}}{d_{\text{LOS}} + 2d_1}\right). \tag{4}$$

From (4), one can easily observe that the magnitude of $r(t)$ can be maximized when the phases of multipath components (direct and reflected signals) are perfectly aligned, that is, by adjusting the time-varying RIS phase as $\theta(t) = -4\pi f_D t \pmod{2\pi}$. We note that the maximization of $|r(t)|$ can only be feasible with a unique RIS, which can adjust its reflection phase in a dynamic manner with respect to time, in accordance with the user movement. The practical issues related to this adjustment procedure are discussed in **Supplementary Material**. With the determined value of $\theta(t)$ discussed above, the complex envelope of the received signal simplifies to

$$r(t) = \frac{\lambda e^{-j2\pi f_D t}}{4\pi}\left(\frac{1}{d_{\text{LOS}}} + \frac{1}{d_{\text{LOS}} + 2d_1}\right). \tag{5}$$

As seen from (5), the magnitude of the complex envelope is now maximized. Furthermore, it remains constant with respect to time can be given in the following:

$$|r(t)|_{\max} = \frac{\lambda}{4\pi}\left(\frac{1}{d_{\text{LOS}}} + \frac{1}{d_{\text{LOS}} + 2d_1}\right). \tag{6}$$

In light of (5) and (6), we have the following three remarks.

Remark 1: The multipath fading effect (rapid fluctuations in the received signal strength) can be eliminated by time-varying intelligent reflection of the RIS for the scenario of **Figure 1**. In this case, we obtain a constant magnitude for the received complex envelope, which is also shown in **Figure 4A**. In other words, by utilizing a unique RIS with a time-varying reflection

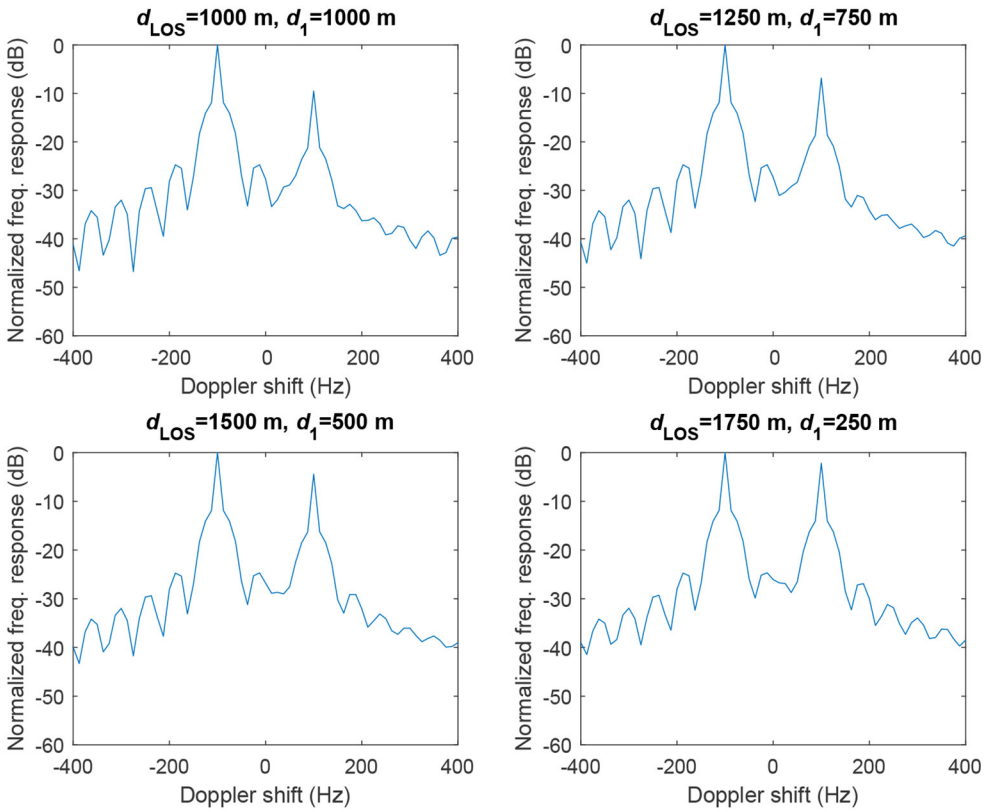

FIGURE 3 | Doppler spectrum of the received signal for varying d_{LOS} and d_1 (FFT size: 256, sampling distance: $\lambda/32 = 0.003125$ m, sampling time: $\lambda/(32 \times V) = 0.3125$ ms).

phase, one can escape from rapid fluctuations in the received signal due to the user movement. For this setup, the position of the RIS can be arbitrarily selected as long as the RIS is adjusting the reflection phase in real-time. We further note that a maximized complex envelope magnitude improves the received signal-to-noise-ratio, in return, the achievable capacity.

Remark 2: The received signal is still subject to a Doppler shift of $-f_D$ Hz, which is also observed from the Doppler spectrum of **Figure 4B**. Although the RIS effectively eliminates fade patterns, due to the direct signal received from the BS, which is out of the control of the RIS, it is not possible to eliminate Doppler frequency shifts in this propagation scenario.

Remark 3: For the case of a practical RIS in which the incoming signals are scattered with many number of tiny RIS elements in **Figure 1**, the received complex envelope is obtained as

$$r(t) = \frac{\lambda}{4\pi d_{\text{LOS}}} e^{-j2\pi d_{\text{LOS}}(t)/\lambda} + \sum_{n=1}^{N} \frac{\lambda^2 G_e}{(4\pi)^2 (d_{\text{LOS}} + d_1) d_1} e^{j(\theta_n(t) - 2\pi d_{R_n}(t)/\lambda)} \tag{7}$$

where G_e is the element gain, $\theta_n(t)$ is the adjustable phase of the nth RIS element and $d_{R_n}(t)$ is the associated path length (Basar and Yildirim, 2020b). Here, under the case of far-field, the same path loss is assumed for all RIS elements. By carefully adjusting the RIS phases, that is, for $\theta_n(t) = 2\pi(d_{R_n}(t) - d_{\text{LOS}}(t))/\lambda$, the signals coming from the RIS can be aligned to the LOS signal and the magnitude of the complex envelope can be kept constant. Please note that by carefully positioning the RIS and adjusting its size, the magnitude of the complex envelope can be maximized by overcoming the multiplicative path loss in (7). In other words, the maximization of the received complex envelope, as well as the effectiveness of the RIS, is not only dependent on time-varying RIS phases, but also its position relative to the transmitter and/or MS due to the multiplicative path loss in (7). Due to the broad scope of the current paper, detailed investigation of RISs with many scattering elements is left as a future study, while the presented results can be generalized in a systematic way.

2.3. Increasing Fading and Doppler Effects With an RIS

So far, we focused our attention on the maximization of the received signal strength for the scenario of **Figure 1**, by carefully adjusting the RIS reflection phase in real time. On the contrary, it might be possible to intentionally degrade the received signal strength as well as increase the Doppler spread for an unintended mobile receiver or for an eavesdropper. Based on the received signal model of (4), when the received two signals are in-phase, we obtain the maximum magnitude for the received signal as

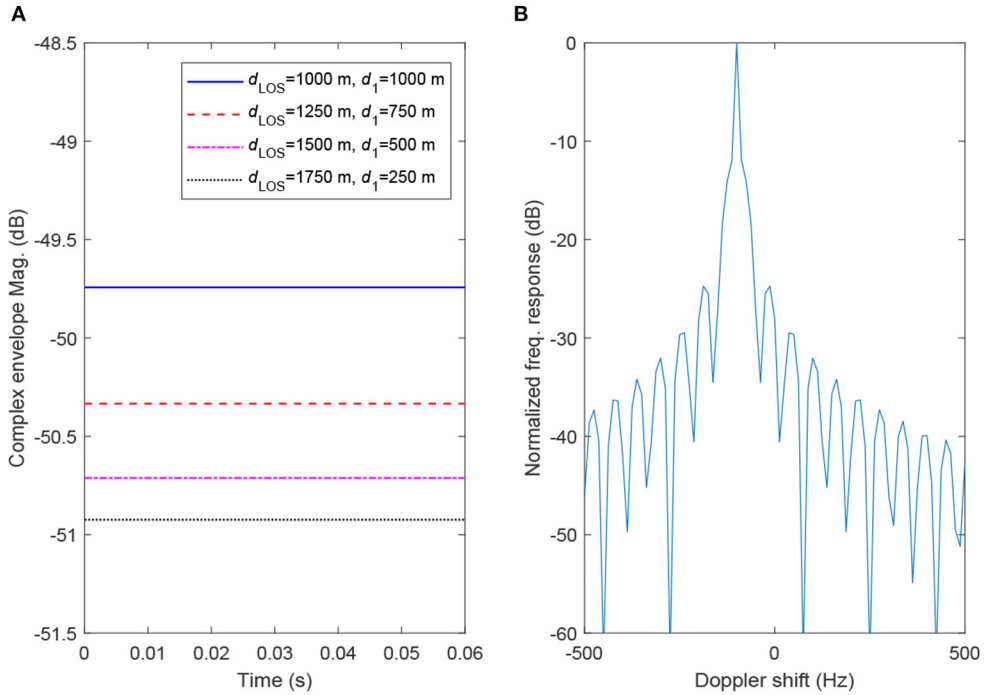

FIGURE 4 | (A) Maximized magnitude of the received signal in the presence of an RIS, **(B)** Doppler spectrum of the received signal for all scenarios.

in (6). On the other hand, adjusting the RIS reflection phase as $\theta(t) = -4\pi f_D t + \pi \pmod{2\pi}$, we obtain completely out-of-phase two arriving signals, and the resulting minimum complex envelope magnitude becomes

$$|r(t)|_{\min} = \frac{\lambda}{4\pi}\left(\frac{1}{d_{\text{LOS}}} - \frac{1}{d_{\text{LOS}} + 2d_1}\right). \tag{8}$$

As seen from (8), the degradation in the received signal strength would be more noticeable for smaller d_1. However, the magnitude of the complex envelope becomes constant as in (6), i.e., no fade patterns are observed. In **Figure 5A**, we depict the minimized complex envelope magnitudes by intentionally out-phasing the direct and reflected signals for varying d_{LOS} and d_1. Comparing **Figures 4A**, **5A**, we observe up to 9 dB degradation in magnitude (for $d_{\text{LOS}} = 1,750$ m and $d_1 = 250$ m), which corresponds to a power variation of 18 dB. In other words, it is possible to enable up to 18 dB variation in the received signal power by deliberately co-phasing and out-phasing the multipath components in the considered setup. It is worth noting that the normalized Doppler spectrum in **Figure 5B** is the same as that of **Figure 4B**.

As another extreme application of an RIS, the Doppler spread can be increased by intentionally increasing the Doppler shift of the reflected signal by $\theta(t) = 2\pi(\tilde{f}_D - f_D)t \pmod{2\pi}$, where $\tilde{f}_D$ is the desired Doppler shift for the reflected signal. Here, a maximum desired Doppler shift of $0.5f_s$ Hz can be observed in simulation, where f_s is the sampling frequency for the continuous-wave signal. In **Figure 6**, we present the magnitude of the complex envelope as well as the Doppler spectrum for the case of $d_{\text{LOS}} = 1,500$ m and $d_1 = 500$ m by carefully adjusting the reflection phase to increase the Doppler spread (reduce the coherence time) by $\tilde{f}_D = 200$ and 400 Hz. As seen from **Figure 6**, an RIS can create new components in the Doppler spectrum, which results in a faster fade pattern for the complex envelope.

Going one step further, we consider the concept of random phase shifts by the RIS, in which the reflection phase is selected at random between 0 and 2π in each time interval. We illustrate the magnitude of the complex envelope and the Doppler spectrum in **Figure 7** for the case random reflection phases, where the reflection phase is selected at random in each sampling time for $d_{\text{LOS}} = 1,500$ m and $d_1 = 500$ m. As seen from **Figures 7A,B**, although the effect in Doppler spectrum is not very significant, it would be possible to obtain a very fast fade pattern in time. Specifically, around 5 dB magnitude variations are observed within a sampling distance of $\lambda/32$ m. It would be possible to obtain an ultra-fast fade pattern by alternating the reflection phase between $\theta(t) = -4\pi f_D t + \pi \pmod{2\pi}$ and $\theta(t) = -4\pi f_D t \pmod{2\pi}$ in each time interval and this is left for interested readers.

3. ELIMINATING DOPPLER EFFECTS THROUGH INTELLIGENT REFLECTION

In this section, we focus on a simple scenario in which the direct link is blocked by an obstacle while the communication between

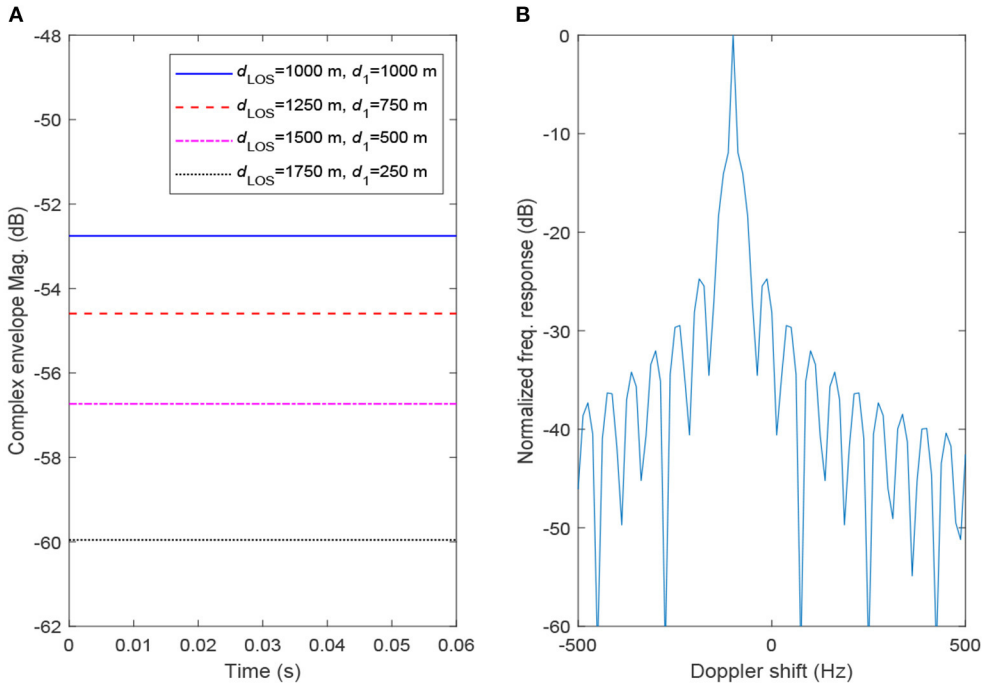

FIGURE 5 | (A) Minimized magnitude of the received signal in the presence of an RIS, **(B)** Doppler spectrum of the received signal for all scenarios.

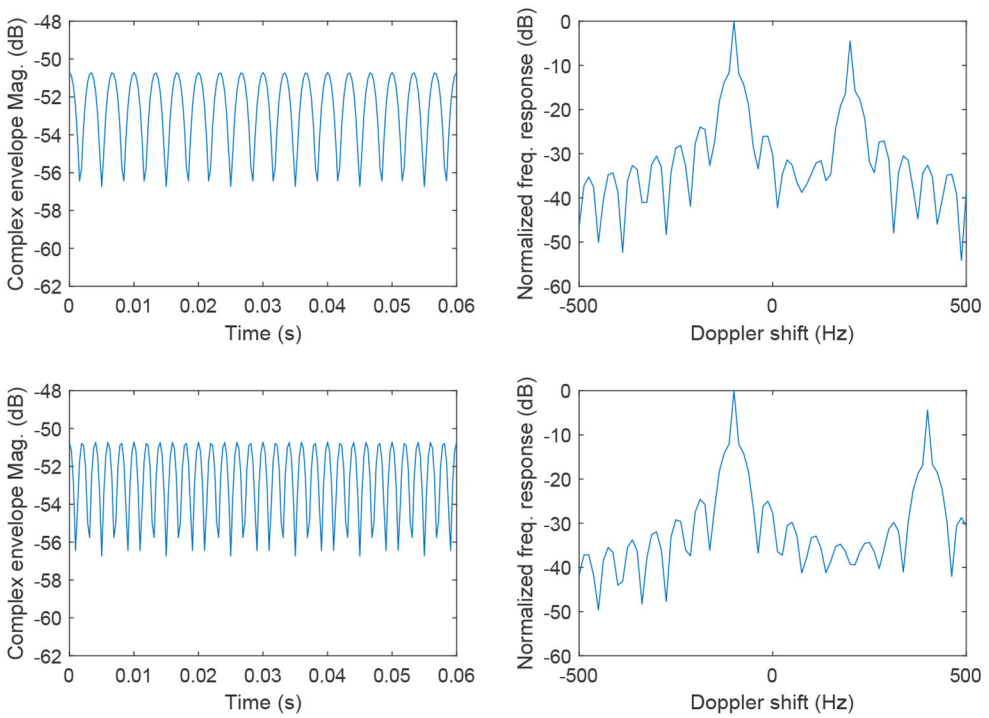

FIGURE 6 | Time varying magnitude and the Doppler spectrum of the received signal with increased Doppler effect for (Top) $\tilde{f}_D = 200$ Hz and (Bottom) $\tilde{f}_D = 400$ Hz.

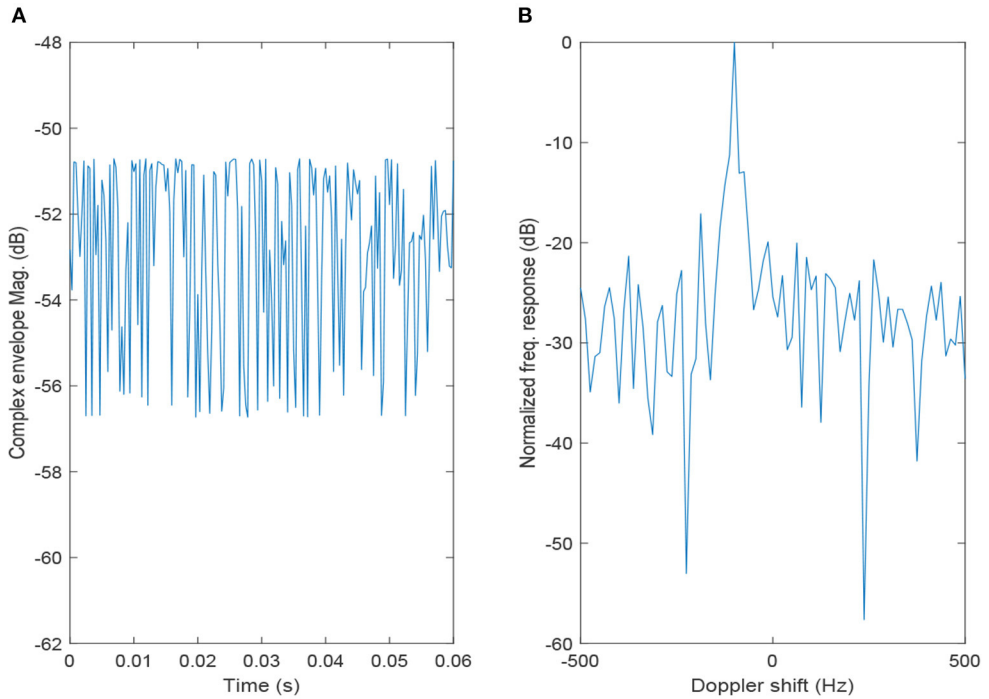

FIGURE 7 | (A) Magnitude of the received signal in the presence of an RIS with random phases, **(B)** Doppler spectrum of the received signal.

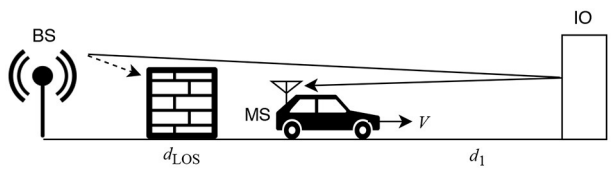

FIGURE 8 | Communications through an IO with a blocked LOS path.

the BS and the MS is established through a reflection from an IO as shown in **Figure 8**. We consider the same assumptions of section II and investigate the Doppler effect on the received signal in the following two cases.

3.1. NLOS Transmission Without an RIS

Under the assumption of specular reflections from the IO with a reflection coefficient of $R = -1$, the received signal can be expressed as

$$r(t) = -\frac{\lambda}{4\pi}\frac{e^{-j\frac{2\pi d_R(t)}{\lambda}}}{d_R(t)} \tag{9}$$

where $d_R(t) = d_{\text{LOS}} + 2d_1 - Vt$ is the time-varying radio path distance for a MS moving with a speed of V m/s. Ignoring the constant phase terms and assuming a very short travel distance, the received signal can be expressed as

$$r(t) = -\frac{\lambda e^{j2\pi f_D t}}{4\pi(d_{\text{LOS}} + 2d_1)}. \tag{10}$$

As seen from (10), since only a single reflection occurs without a LOS signal and other multipath components, the received signal magnitude does not exhibit a fade pattern, that is, fixed with respect to time and given by $|r(t)| = \lambda/(4\pi(d_{\text{LOS}} + d_1))$. However, the received signal is still subject to a Doppler frequency shift of f_D Hz, which is evident from (10), due to the movement of the MS.

3.2. NLOS Transmission With an RIS

Here, we focus on the scenario of **Figure 8** while assuming that the IO is equipped with an RIS that is able to provide adjustable phase shifts, i.e., $R(t) = e^{j\theta(t)}$, as in section II. In this case, the received signal can be expressed as

$$r(t) = \frac{\lambda e^{j2\pi f_D t + j\theta(t)}}{4\pi(d_{\text{LOS}} + 2d_1)}. \tag{11}$$

As seen from (11), the magnitude of the received signal is independent from the reflection phase and the same as the previous case (without an RIS). However, it might be possible to completely eliminate the Doppler effect by adjusting the RIS reflection phase as $\theta(t) = -2\pi f_D t \pmod{2\pi}$. We give the following remark.

Remark 4: When there is no direct transmission between the BS and the MS over which the RIS has no control, intelligent reflection allows one to completely eliminate the Doppler effect,

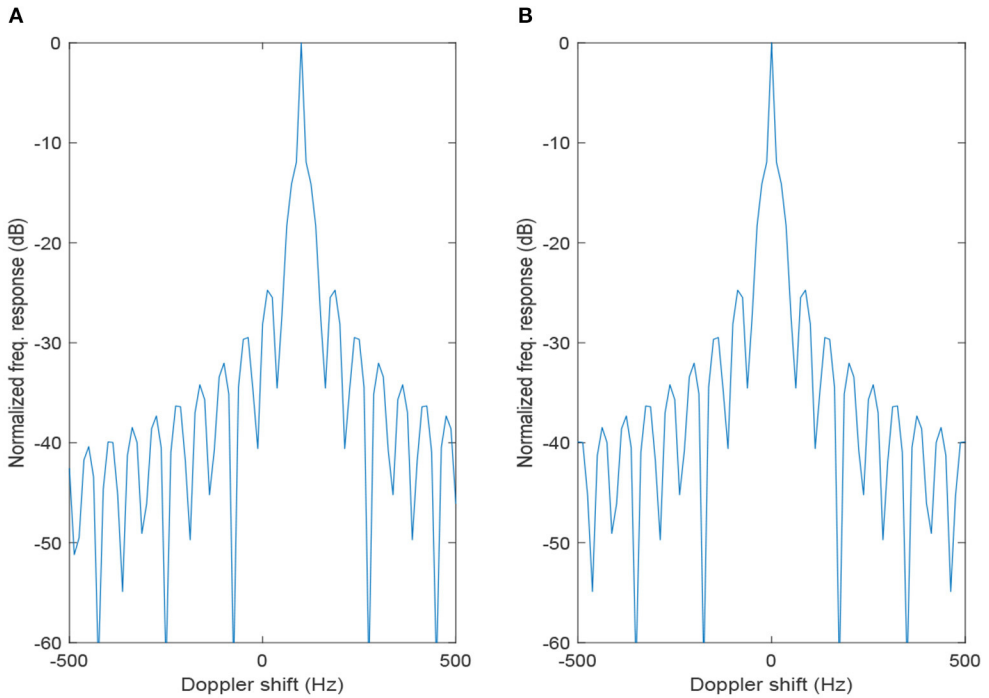

FIGURE 9 | Doppler spectrum of the received signal for the scenario of **Figure 8**: **(A)** without an RIS, **(B)** with an RIS.

TABLE 1 | Comparison of different RIS application scenarios.

Scenario	Figure #	Multipath mitigation	Doppler mitigation	Constant envelope
LOS + RIS	1	Yes	No	Yes
NLOS + RIS	8	n/a	Yes	Yes
LOS + RIS + IO	S1	Yes	No	No
LOS + 2 RISs	S1	Yes	No	Yes
NLOS + 2 RISs	n/a	Yes	Yes	Yes
LOS + *N* RISs + *M* IOs	S6	Yes	No	Yes (approx.)
NLOS + *N* RISs + *M* IOs	n/a	Yes	Yes (approx.)	Yes (approx.)

by carefully compensating the Doppler phase shifts through the RIS.

In **Figure 9**, we show the Doppler spectrum of the received signal with and without an RIS for $d_{\text{LOS}} = d_1 = 1,000$ m. As seen from **Figure 9**, the Doppler effect is eliminated (0 Hz) by adjusting the RIS reflections accordingly.

As discussed earlier, it is not possible the modify the magnitude of the complex envelope with an RIS for the scenario of **Figure 8**, however, as done in section II, the Doppler spread can be enhanced by $\theta(t) = 2\pi(\tilde{f}_D - f_D)t \pmod{2\pi}$, where $\tilde{f}_D$ is the desired Doppler frequency. The observation of the resulting spectrum is straightforward and left for the interested readers.

4. CONCLUSIONS AND FUTURE WORK

In this paper, we have revisited the multipath fading phenomenon of mobile communications and provided unique solutions by utilizing the emerging concept of RISs in the presence of Doppler effects. By following a bottom-up approach, first, we have investigated simple propagation scenarios with a single RIS and/or a plain IO. Then we have developed several novel methods for the case of multiple RISs and plain IOs depending on the their total numbers as well as the presence of the LOS path. Finally, we have considered a number of practical issues, including erroneous estimation of Doppler shifts, practical reflection phases, and discrete-time reflection phases, for the target setups and evaluated the overall performance under these imperfections. In **Table 1**, we summarize the main insights derived in this work for different RIS application scenarios.

One of the most important conclusions of this paper is that the multipath fading effect caused by the movement of the mobile receiver/transmitter can be effectively eliminated and/or mitigated by real-time tunable RISs. A number of interesting trade-offs have been demonstrated between fade pattern elimination and complex envelope magnitude maximization. While this work sheds light on the development of RIS-assisted mobile networks, exploration of amplitude/phase modulations and more practical path loss/propagation models appear as interesting future research directions.

DATA AVAILABILITY STATEMENT

The original contributions presented in the study are included in the article/**Supplementary Material**, further inquiries can be directed to the corresponding author/s.

AUTHOR CONTRIBUTIONS

The author confirms being the sole contributor of this work and has approved it for publication.

FUNDING

This work was supported by TUBITAK under 120E401.

SUPPLEMENTARY MATERIAL

The Supplementary Material for this article can be found online at: https://www.frontiersin.org/articles/10.3389/frcmn.2021.672857/full#supplementary-material

REFERENCES

Abeywickrama, S., Zhang, R., and Yuen, C. (2020). "Intelligent reflecting surface: practical phase shift model and beamforming optimization," in *Proceedings of IEEE International Conference on Communications (ICC)*. doi: 10.1109/ICC40277.2020.9148961

Badiu, M. A., and Coon, J. P. (2020). Communication through a large reflecting surface with phase errors. *IEEE Wireless Commun. Lett*. 9, 184–188. doi: 10.1109/LWC.2019.2947445

Basar, E. (2016). Index modulation techniques for 5G wireless networks. *IEEE Commun. Mag*. 54, 168–175. doi: 10.1109/MCOM.2016.7509396

Basar, E. (2019a). Media-based modulation for future wireless systems: a tutorial. *IEEE Wireless Commun*. 26, 160–166. doi: 10.1109/MWC.2019.1800568

Basar, E. (2019b). "Transmission through large intelligent surfaces: a new frontier in wireless communications," in *Proceedings of European Conference on Networks and Communications (EuCNC 2019)* (Valencia). doi: 10.1109/EuCNC.2019.8801961

Basar, E. (2020). "Beyond massive MIMO: reconfigurable intelligent surface-assisted wireless communications," in *Flexible and Cognitive Radio Access Technologies for 5G and Beyond, Chapter 10*, eds H. Arslan and E. Basar (Stevenage Herts: IET), 317–338. doi: 10.1049/PBTE092E_ch10

Basar, E., Renzo, M. D., de Rosny, J., Debbah, M., Alouini, M. S., and Zhang, R. (2019). Wireless communications through reconfigurable intelligent surfaces. *IEEE Access* 7, 116753–116773. doi: 10.1109/ACCESS.2019.2935192

Basar, E., Wen, M., Mesleh, R., Renzo, M. D., Xiao, Y., and Haas, H. (2017). Index modulation techniques for next-generation wireless networks. *IEEE Access* 5, 16693–16746. doi: 10.1109/ACCESS.2017.2737528

Basar, E., and Yildirim, I. (2020a). Indoor and Outdoor Physical Channel Modeling and Efficient Positioning for Reconfigurable Intelligent Surfaces in mmWave Bands. *arXiv* [Under review]. Available online at: https://arxiv.org/abs/2006.02240

Basar, E., and Yildirim, I. (2020b). "SimRIS channel simulator for reconfigurable intelligent surface-empowered communication systems," in *Proceedings of IEEE Latin-American Conference on Communications*. doi: 10.1109/LATINCOM50620.2020.9282349

Basar, E., and Yildirim, I. (2020c). Reconfigurable intelligent surfaces for future wireless networks: a channel modeling perspective. *IEEE Wireless Commun*. 1–7. doi: 10.1109/MWC.001.2000338

Chen, J., Liang, Y. C., Pei, Y., and Guo, H. (2019). Intelligent reflecting surface: a programmable wireless environment for physical layer security. *IEEE Access* 7, 82599–82612. doi: 10.1109/ACCESS.2019.2924034

Cui, M., Zhang, G., and Zhang, R. (2019). Secure wireless communication via intelligent reflecting surface. *IEEE Wireless Commun. Lett*. 8, 1410–1414. doi: 10.1109/LWC.2019.2919685

Cui, T. J., Qi, M. Q., Wan, X., Zhao, J., and Cheng, Q. (2014). Coding metamaterials, digital metamaterials and programmable metamaterials. *Light Sci. Appl*. 3:e218. doi: 10.1038/lsa.2014.99

Dai, J. Y., Tang, W., Chen, M. Z., Chan, C. H., Cheng, Q., Jin, S., et al. (2021). Wireless communication based on information metasurfaces. *IEEE Trans. Microwave Theor. Tech*. 69, 1493–1510. doi: 10.1109/TMTT.2021.3054662

Dai, L., Wang, B., Wang, M., Yang, X., Tan, J., Bi, S., et al. (2020). Reconfigurable intelligent surface-based wireless communications: antenna design, prototyping, and experimental results. *IEEE Access* 8, 45913–45923. doi: 10.1109/ACCESS.2020.2977772

Danufane, F. H., Di Renzo, M., de Rosny, J., and Tretyakov, S. (2020). On the Path-Loss of Reconfigurable Intelligent Surfaces: An Approach Based on Green's Theorem Applied to Vector Fields. *arXiv* [Under review].

Di Renzo, M. (2019). Smart radio environments empowered by reconfigurable AI meta-surfaces: an idea whose time has come. *EURASIP J. Wireless Commun. Net*. 2019:129. doi: 10.1186/s13638-019-1438-9

Di Renzo, M., Zappone, A., Debbah, M., Alouini, M. S., Yuen, C., de Rosny, J., et al. (2020). Smart radio environments empowered by reconfigurable intelligent surfaces: How it works, state of research, and the road ahead. *IEEE J. Select. Areas Commun*. 38, 2450–2525. doi: 10.1109/JSAC.2020.3007211

Ding, Y., Kim, K. J., Koike-Akino, T., Pajovic, M., Wang, P., and Orlik, P. (2017). Spatial scattering modulation for uplink millimeter-wave systems. *IEEE Commun. Lett*. 21, 1493–1496. doi: 10.1109/LCOMM.2017.2684126

Ding, Z., and Poor, H. V. (2019). A simple design of IRS-NOMA transmission. *IEEE Commun. Lett*. 24, 1119–1123. doi: 10.1109/LCOMM.2020.2974196

Ellingson, S. (2019). Path Loss in Reconfigurable Intelligent Surface-Enabled Channels. *arXiv* [Under review].

Fontan, F. P., and Espineira, P. M. (2008). *Modeling the Wireless Propagation Channel: A Simulation Approach with MATLAB*. West Sussex: Wiley.

Fu, M., Zhou, Y., and Shi, Y. (2019). "Intelligent reflecting surface for downlink non-orthogonal multiple access networks," in *2019 IEEE Globecom Workshops (GC Wkshps)* (Waikoloa, HI). doi: 10.1109/GCWkshps45667.2019.9024675

Gatherer, A. (2018). *What Will 6G Be?* Available online at: https://www.comsoc.org/publications/ctn/what-will-6g-be

He, Z. Q., and Yuan, X. (2020). Cascaded channel estimation for large intelligent metasurface assisted massive MIMO. *IEEE Wireless Commun. Lett*. 9, 210–214. doi: 10.1109/LWC.2019.2948632

Huang, C., Alexandropoulos, G. C., Zappone, A., Debbah, M., and Yuen, C. (2018a). "Energy efficient multi-user MISO communication using low resolution large intelligent surfaces," in *Proceedings of IEEE Global Communications Conference* (Abu Dhabi). doi: 10.1109/GLOCOMW.2018.8644519

Huang, C., Zappone, A., Alexandropoulos, G. C., Debbah, M., and Yuen, C. (2019). Reconfigurable intelligent surfaces for energy efficiency in wireless communication. *IEEE Trans. Wireless Commun*. 18, 4157–4170. doi: 10.1109/TWC.2019.2922609

Huang, C., Zappone, A., Debbah, M., and Yuen, C. (2018b). "Achievable rate maximization by passive intelligent mirrors," in *Proceedings of 2018 IEEE International Conference on Acoustics, Speech and Signal Processing (ICASSP)* (Calgary, AB), 3714–3718. doi: 10.1109/ICASSP.2018.8461496

Kaina, N., Dupré, M., Lerosey, G., and Fink, M. (2014). Shaping complex microwave fields in reverberating media with binary tunable metasurfaces. *Sci. Rep*. 4:6693. doi: 10.1038/srep06693

Khandani, A. K. (2013). "Media-based modulation: a new approach to wireless transmission," in *Proceedings of IEEE International Symposium on Information Theory* (Istanbul), 3050–3054. doi: 10.1109/ISIT.2013.6620786

Liaskos, C., Nie, S., Tsioliaridou, A., Pitsillides, A., Ioannidis, S., and Akyildiz, I. (2018). A new wireless communication paradigm through software-controlled metasurfaces. *IEEE Commun. Mag*. 56, 162–169. doi: 10.1109/MCOM.2018.1700659

Liu, F., Tsilipakos, O., Pitilakis, A., Tasolamprou, A. C., Mirmoosa, M. S., Kantartzis, N. V., et al. (2019). Intelligent metasurfaces with continuously tunable local surface impedance for multiple reconfigurable functions. *Phys. Rev. Appl*. 11:044024. doi: 10.1103/PhysRevApplied.11.044024

Mishra, D., and Johansson, H. (2019). "Channel estimation and low-complexity beamforming design for passive intelligent surface assisted MISO wireless energy transfer," in *Proceedings of 2019 IEEE International Conference on Acoustics, Speech and Signal Processing (ICASSP)* (Brighton). doi: 10.1109/ICASSP.2019.8683663

Molisch, A. F. (2011). *Wireless Communications*. West Sussex, UK: Wiley.

Nadeem, Q. U. A., Kammoun, A., Chaaban, A., Debbah, M., and Alouini, M. S. (2020). Asymptotic max-min SINR analysis of reconfigurable intelligent surface assisted MISO systems. *IEEE Trans. Wireless Commun*. 19, 7748–7764. doi: 10.1109/TWC.2020.2986438

Saad, W., Bennis, M., and Chen, M. (2020). A vision of 6G wireless systems: applications, trends, technologies, and open research problems. *IEEE Netw*. 34, 134–142. doi: 10.1109/MNET.001.1900287

Subrt, L., and Pechac, P. (2012a). "Controlling propagation environments using intelligent walls," in *Proceedings of 2012 6th European Conference on Antennas and Propagation (EUCAP)* (Prague), 1–5. doi: 10.1109/EuCAP.2012.6206517

Subrt, L., and Pechac, P. (2012b). Intelligent walls as autonomous parts of smart indoor environments. *IET Commun*. 6, 1004–1010. doi: 10.1049/iet-com.2010.0544

Taha, A., Alrabeiah, M., and Alkhateeb, A. (2021). Enabling large intelligent surfaceswith compressive sensing and deep learning. *IEEE Access* 9, 44304–44321.

Tan, X., Sun, Z., Jornet, J. M., and Pados, D. (2016). "Increasing indoor spectrum sharing capacity using smart reflect-array," in *Proceedings of 2016 IEEE International Conference on Commununications (ICC)* (Kuala Lumpur), 1–6. doi: 10.1109/ICC.2016.7510962

Tan, X., Sun, Z., Koutsonikolas, D., and Jornet, J. M. (2018). "Enabling indoor mobile millimeter-wave networks based on smart reflect-arrays," in *Proceedings of IEEE Conference on Computer Communications (INFOCOM)* (Honolulu, HI), 270–278. doi: 10.1109/INFOCOM.2018.8485924

Tang, W. (2019). Wireless Communications with reconfigurable intelligent surface: path loss modeling and experimental measurement. *IEEE Trans. Wireless Commun*. 20, 421–439. doi: 10.1109/TWC.2020.3024887

Wu, Q., and Zhang, R. (2018). "Intelligent reflecting surface enhanced wireless network: joint active and passive beamforming design," in *Proceedings of IEEE Global Communication Conference* (Abu Dhabi). doi: 10.1109/GLOCOM.2018.8647620

Wu, Q., and Zhang, R. (2019a). "Beamforming optimization for intelligent reflecting surface with discrete phase shifts," in *Proceedings of 2019 IEEE International Conference on Acoustics, Speech and Signal Processing (ICASSP)* (Brighton). doi: 10.1109/ICASSP.2019.8683145

Wu, Q., and Zhang, R. (2019b). Towards smart and reconfigurable environment: intelligent reflecting surface aided wireless network. *IEEE Commun. Mag*. 58, 106–112. doi: 10.1109/MCOM.001.1900107

Wu, Q., Zhang, S., Zheng, B., You, C., and Zhang, R. (2020). Intelligent reflecting surface aided wireless communications: a tutorial. *IEEE Trans. Commun*. doi: 10.1109/TCOMM.2021.3051897

Xiong, X., Chan, J., Yu, E., Kumari, N., Sani, A. A., Zheng, C., et al. (2017). "Customizing indoor wireless coverage via 3D-fabricated reflectors," in *Proceedings of 4th ACM International Conference on Systems for Energy-Efficient Built Environments* (Delft), 1–10. doi: 10.1145/3137133.3137148

Yang, H., Cao, X., Yang, F., Gao, J., Xu, S., Li, M., et al. (2016). A programmable metasurface with dynamic polarization, scattering and focusing control. *Sci. Rep*. 6:35692. doi: 10.1038/srep35692

Yildirim, I., Uyrus, A., and Basar, E. (2020). Modeling and analysis of reconfigurable intelligent surfaces for indoor and outdoor applications in future wireless networks. *IEEE Trans. Commun*. 69, 1290–1301. doi: 10.1109/TCOMM.2020.3035391

Yu, X., Xu, D., and Schober, R. (2019a). "Enabling secure wireless communications via intelligent reflecting surfaces," in *Proceedings of IEEE Global Communication Conference (GLOBECOM)* (Waikoloa, HI). doi: 10.1109/GLOBECOM38437.2019.9014322

Yu, X., Xu, D., and Schober, R. (2019b). "MISO wireless communication systems via intelligent reflecting surfaces," in *2019 IEEE/CIC International Conference on Communications China (ICCC)* (Changchun). doi: 10.1109/ICCChina.2019.8855810

Conflict of Interest: The author declares that the research was conducted in the absence of any commercial or financial relationships that could be construed as a potential conflict of interest.